Molecular Dynamics Simulation Study on Segmental Motion in Liquid Normal Heptadecane

Song Hi Lee*, Han Soo Kim†, and Hyungsuk Pak‡

Department of Chemistry, Kyungsung University, Pusan 608-736, Korea
†Department of Industrial Chemistry, Kangnung National University, Kangnung 212-702, Korea
‡Department of Chemistry, Seoul National University, Seoul 151-740, Korea
Received July 18, 1998

We present results of molecular dynamic (MD) simulations for the segmental motion of liquid *n*-heptadecane in order to investigate conformational transitions from one rotational isomeric state to another. The behavior of the hazard plots for *n*-heptadecane obtained from our MD simulations are compared with that for polymer of Brownian dynamics (BD) study. The transition rate at the ending dihedrals of the *n*-heptadecane chain is much higher than that at the central dihedrals. In the study of correlation between transitions of neighboring dihedrals, the large value of c_2 implies that some 30% of the transitions of the second neighbors can be regarded as following transitions two bonds away in a correlated fashion. Finally the analysis of multiple transitions and the number of times occurred in the initial 0.005 ns are discussed.

Introduction

Recently, there have been considerable experimental and theoretical efforts in order to elucidate the dynamics of molecular conformational motions in solution. These motions have been studied by such techniques as NMR, dielectric relaxation, ultrasonic attenuation, dynamical light scattering, fluorescence depolarization, and excimer fluorescence. However, these experiments may not reveal many of the details about the motion, such as whether correlation exists between transitions of near neighbors, or, in general, what the effect of the rest of the chain is on the bond undergoing transitions. Computer simulation of the structural formation of polymer chains has become the focus of attention in physics, chemistry, and material science. Intensive studies of various model polymer systems[1-7] have been made in order to understand the dynamics of conformational transitions.

When one bond in a long chain of a polymer in solution undergoes a conformational transition, if there is no accompanying transition of any bonds of the tails, the tails' positions in space after the transition differ markedly from the initial positions. The bond undergoes a large rotational displacement which induces a large solvent frictional resistance. There are certain modes of motion (so-called crankshaft), such as the Schatzki crankshaft[8] or the three-body motion,[9] which leave the tails in the same position at the start and end of the transition. Such motions involve two barrier crossings, or the passage through some fairly high energy intermediate state.

In the early study for kinetics of conformational transitions in chain molecules, Skolnick and Helfand[1] classified the conformational transitions in the chain molecules into three types as shown in Figure 1. The first is the so-called type 1 or crankshaft motions wherein several conformational transitions occur close together in space and time, in such a way that there is no net motion of the attached tails. Historically, the first crankshaft considered was the Schatzki crankshaft[8] picture. Another type 1 motion is the three-bond motion[9] in Figure 1(a). Every time one has a *gauche* bond in a chain, that bond and its neighbors on each side form half a cyclohexane ring. A motion in which these bonds flip to the other half of the cyclohexane ring clearly leaves the tails in the same position finally that they were in initially. The activation energy of this type of motion must be large since it involves the energy of at least two barrier crossings plus the solvent friction.

There is another type of multiple transition in which the polymer tails do not have to swing, but they do translate. Every time there is a *trans* bond in the chain, the two attached bonds are parallel. If one of these two parallel bonds undergoes a rotation $+\Delta\phi$ while the other rotates $-\Delta\phi$, then the tails translate but not rotate. Figures 1(b) and (c) show two kinds of type 2 motion - *gauche* migration (*tttgt* → *tgttt*) and pair *gauche* production (*ttttt* → tg^+tg^-t). In type 3 transitions, called isolated transitions, relative orientation of one end of the segment undergoing transition changes with respect to the other end as a result of this transition but these transitions may not be considered as complete conformational changes in the usual sense. They are just temporal distortions of the stable conformations lasting for very short time interval which in most cases simply return to original equilibrium conformations (Figure 1(d)). This is the motivation for the careful examination of such motions in the present paper.

In a recent paper,[10] we carried out molecular dynamics (MD) simulations for the segmental motion of normal butane as the base case for a consistent study of conformational transitions from one rotational isomeric state to another in long chains of liquid *n*-alkanes. In the present paper the same technique is applied to study the segmental motion of normal heptadecane in order to investigate conformational transitions in long chains of liquid *n*-heptadecanes. The paper is organized as follows. Section II contains a brief description of molecular models and molecular dynamics simulation methods followed by Section III which presents the results of our simulations and Section IV where our conclusions are summarized.

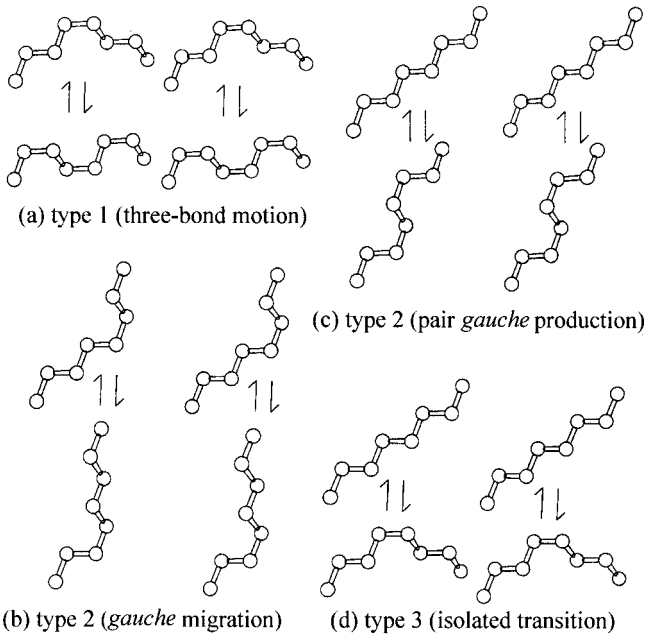

(a) type 1 (three-bond motion)

(c) type 2 (pair *gauche* production)

(b) type 2 (*gauche* migration)

(d) type 3 (isolated transition)

Figure 1. Type 1, 2, and 3 of conformational transitions in a chain molecule.

Molecular Model and Molecular Dynamics Simulations

In the present study, we have carried out MD simulations of liquid *n*-heptadecane at various temperatures using an expanded collapsed atomic model.[11-13] Each simulation was carried out in the NVT ensemble; the density and hence the length of cubic simulation box were fixed (N=27 and ρ= 0.782 g/cc). The usual periodic boundary condition in the x-, y-, and z-directions and minimum image convention for pair potential were applied. A spherical cut-off of radius R_c=2.5 σ, where σ is the LJ parameter, was employed for all the pair interactions. Gaussian isokinetics[14,15] was used to keep the temperature of the system constant.

The molecular model adopted for *n*-heptadecane is so called the expanded collapsed atomic model. Monomeric units are treated as single spheres with masses of 14.145 g/mole. They interact through an LJ potential between the spheres in different molecules and between the spheres more than three apart on the same molecule. The C-C-C-C torsional rotational potential is given by the original Ryckaert-Bellemans form[16]:

$$V(\phi) = c_0 + c_1\cos\phi + c_2\cos^2\phi + c_3\cos^3\phi + c_4\cos^4\phi + c_5\cos^5\phi \quad (1)$$

where ϕ is the C-C-C-C dihedral angle. The LJ parameters and c_i's are listed in Table 1. There are actually five independent constants in this potential, which may be specified: the height of the *trans-gauche* barrier, E_{tg}*=12.340 kJ/mole; the energy difference between the *trans* and *gauche* minima, E_g=2.938 kJ/mole (and E_{gt}*=9.402 kJ/mole); the energy at the *cis* state, E_{cis}=44.818 kJ/mole; the angular location of the barrier, $\phi^*=\pm 60°$; and the angular location of the *gauche* minimum, $\phi_g=\pm 120°$.

This model also includes the C-C bond stretching and C-C-C bond angle bending potentials in addition to the LJ and torsional potentials of the above Ryckaert-Bellemans potential:

Table 1. Potential parameters for liquid *n*-heptadecane

LJ parameters	σ(nm)	ε(kJ/mol)			
C-C	0.3923	0.5986			
torsional	c_o(kJ/mol)	c_1	c_2	c_3	c_4	c_5
C-C-C-	9.279	12.136	-13.120	-3.060	26.240	-31.495
bond stretching		r_e(nm)		K_o(kJ/mol·nm^2)		
C-C		0.153		132600		
bond angle bending		θ_e(deg)	K_1(kJ/mol·deg^2)		K_2(kJ/mol·deg^3)	
C-C-C		109.47	0.05021		0.000482	

$$V_b(r_{ij}) = K_0(r_{ij} - r_e)^2 \quad (2)$$

$$V_a(\theta) = K_1(\theta - \theta_e)^2 - K_2(\theta - \theta_e)^3 \quad (3)$$

The equilibrium bond length (r_e) and bond angle (θ_e), and the force constants (K_o, K_1, and K_2) are used by Chynoweth *et al.*[11-13] which are originally provided by the work of White and Boville,[17] and are given in Table 1.

For the integration over time, we adopted Gear's fifth-order predictor-corrector algorithm[18] with a time step of 0.0005 ps. A total of 12,000,000 time steps was simulated each for the average and the configurations of molecules were stored every 10 time steps for further analysis.

Conformational Transition of *n*-heptadecane

The dihedral angle ϕ for a given C-C bond is one of the three states - *gauche*-plus(g^+), *trans*(t), or *gauche*-minus (g^-) by the C-C-C-C torsional rotational potential. When ϕ arrives at the minimum of one of the potential wells, we set a clock equal to zero and count the number of time steps required for the bond to first reach the minimum of the other wells. Then we reset the clock zero and measure the next transition time, etc. The transition times are the first passage times from one minimum to the other. Thus there is obtained a set of n transition times. These are arranged in ascending order, $t_{(1)} \le t_{(2)} \le \cdots \le t_{(n)}$, forming what is called a set of order statistics.

The information contained in the set of first passage times is best depicted in a hazard plot. Let $h(t)$, the hazard rate, be defined such that $h(t)dt$ is the probability that a bond, which has not had a transition in a time t since the last transition, has a transition between t and $t+dt$. Define the cumulative hazard as

$$H(t) = \int_0^t h(t')\,dt'. \quad (4)$$

It is easily shown that the probability, $P(t)$, that a bond has the next transition in a time less than t since the last transition is related to the hazard by

$$P(t) = 1 - \exp[-H(t)] \quad (5)$$

and the probability density of a transition at t is

$$p(t) = dP/dt = h(t)\exp[-H(t)]. \quad (6)$$

The rate measured is a composite of all processes, *trans* going to either one of the *gauches* or vice versa:

$$\lambda = 2p_t \lambda_{tg} + 2p_g \lambda_{gt}. \quad (7)$$

where λ_{tg} is the rate of transition from *trans* to one of the *gauches*, λ_{gt} is the reverse rate, p_t is the fraction of *trans*, and p_g is the fraction of one of the *gauche* states. Detailed balance requires that

$$p_t \lambda_{tg} = p_g \lambda_{gt}. \quad (8)$$

so that

$$\lambda_{tg} = \lambda/(4p_t). \quad (9)$$

In Figure 2 we plot hazard plots of the total 14 dihedral angles for *n*-heptadecane molecular dynamics simulations at various temperatures of 296, 266, 236, and 206 K. The plots are straight lines except in the short time regions. The behavior of hazard plots for *n*-heptadecane obtained from our MD simulation is very similar to that of polymer conformation transition in a Brownian dynamics [BD] study[3] but the fractions of transitions that immediately reverse are different (see below). The enhanced transition (*i.e.* the slope) at short time region in the hazard plot of Figure 2 is very small when compared with the hazard plot for *n*-butane of MD study[10] but the fractions of transitions that immediately reverse are almost the same. Note that there is no enhanced transition at short time region in the hazard plot for *n*-butane of the BD study.[3] The major reason for the enhanced short time transition rate in the polymer conformation may appear to be that when a transition occurs the neighbors may not be in, or relax into, a position which can accept this new conformation. If the first transition was $t \rightarrow g^{\pm}$, the second is almost always the reverse since the *cis* barrier is quite high. But $g^{\pm} \rightarrow t$ can be followed either the reverse or by $t \rightarrow g^{\mp}$. The fractions for which the first state is *gauche* and goes back to the same *gauche* are 50.2, 49.0, 48.5, and 56.3% at 206, 236, 266 and 296 K, respectively. This results is much different from 90.6% of $g^{\pm} \rightarrow t \rightarrow g^{\pm}$ at 372 K in the explanation for the enhanced short time transition rate inthe polymer conformation transition of the BD study.[3]

In Figure 3 we see hazard plots of some averages over each dihedral at 296 K. The transition rate at the ending dihedrals (38.9 ns^{-1}) of *n*-heptadecane is much higher than

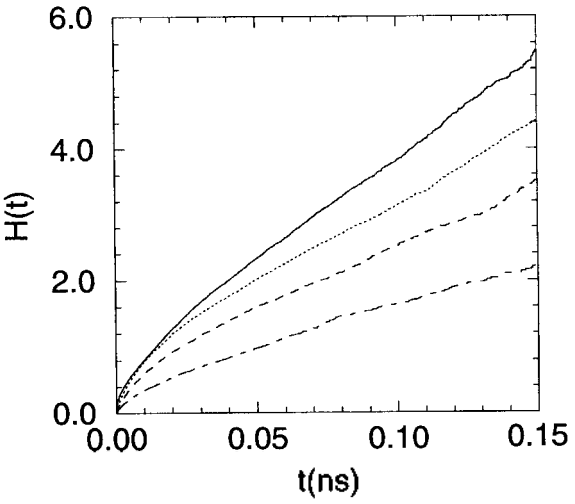

Figure 2. Hazard plots for *n*-heptadecane molecular dynamics simulations at 296 (——), 266 (·····), 236 (-----), and 206 K(-·-·-).

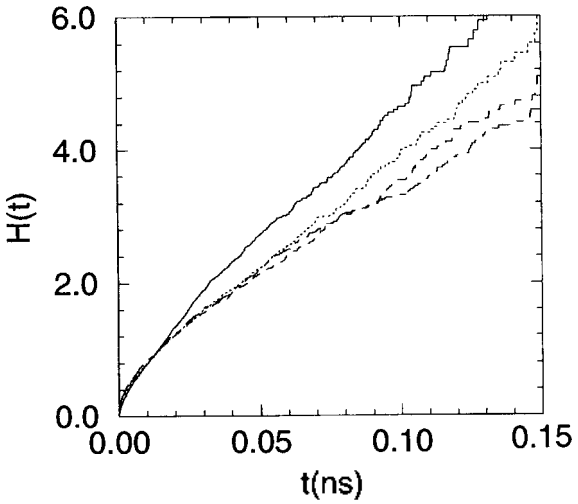

Figure 3. Hazard plots of 1st, 2nd, 13th, and 14th dihedrals (——), 3rd, 4th, 11th, and 12th dihedrals (·····), 5th, 6th, 9th, and 10th dihedrals (-----), and 7th and 8th dihedrals (-·-·-) for *n*-heptadecane molecular dynamics simulations at 296 K.

that at the central dihedrals (23.3 ns^{-1}) at 296 K. As the temperature decreases, the transition rate at the central dihedrals is decreased much faster than that at the ending dihedrals. At the lowest temperature (206 K) we have rarely observed any conformational transition at 5th to 10th dihedrals. The fractions of *trans* at low temperatures are very high as seen in Table 2 which reflects the elongation of the *n*-heptadecane chain with very rare conformational transitions at those temperatures.

In describing the hazard curve, many analytical approximations are possible. We consider only that all the uncompleted reactions which reverse are regarded as reversing instantly and that thereafter the transitions to new states are a Poisson process with rate λ_o. In that case the hazard rate is

$$h(t) = \lambda_o + \nu_o \delta(t-) \quad (10)$$

and the cumulative hazard is

$$H(t) = \lambda_o t + \nu_o. \quad (11)$$

According to Eq. (5), the probability of a transition having occurred in a time less than t is

$$P(t) = 1 - (1 - c_o)\exp[-\lambda_o t], \quad t > 0 \quad (12)$$

$$c_o = 1 - \exp[-\nu_o]. \quad (13)$$

From the fact that P(0+)=c_o we can identify c_o as the fraction of "transitions" that immediately reverse. A measure of c_o can be obtained by fitting the asymptotic portion of the hazard plot with a straight line and using the intercept, ν_o, in

Table 2. Transition rates for *n*-heptadecane at various temperatures

T(K)	λ (ns^{-1})	λ_{tg}	p_t	c_o (%)
296	30.7	10.1	0.760	54.6
266	23.8	6.23	0.956	51.7
236	18.4	4.72	0.975	48.7
206	11.8	3.01	0.980	36.5

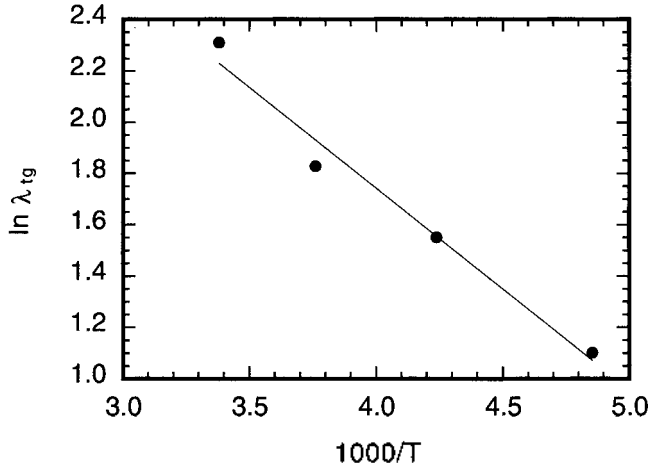

Figure 4. Arrhenius plots of the logarithm of the transition rates *vs.* 1000/T.

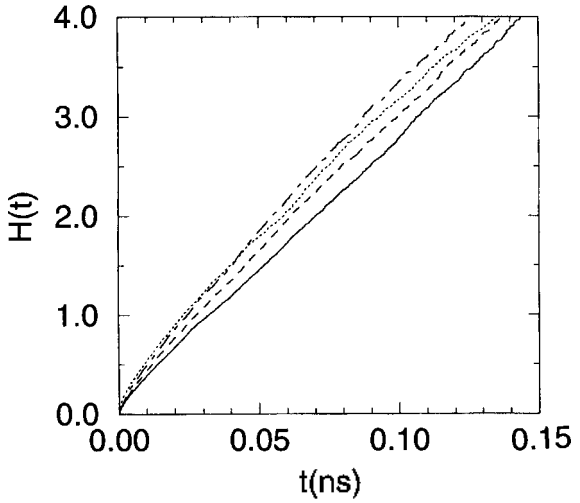

Figure 5. Hazard plots of m=1 (——), m=2 (·····), m=3 (-----), and m=4 (-·-·-) for n-heptadecane molecular dynamics simulations at 296 K.

Eq. (13). The fit has been done by least squares, omitting the data in the short time, severly nonlinear region. The calculated c_o's are listed in Table 2.

The results are reported in Table 2 where the rates λ are calculated from the hazard fit to Eq. (11) by least squares, excluding the short time regions, λ_{tg} is obtained from Eqs. (8) and (9). The transition rates λ_{tg} are given in the form of a prefactor f_{tg} and an activation energy E_{tg}^* defined by

$$\lambda_{tg} = f_{tg} \exp(-E_{tg}^*/kT). \quad (14)$$

An Arrhenius plot of the transition rates from Table 2, Figure 4, give activation energies of $E_{tg}^* \simeq 0.530\ E_{tg}^*$ with f_{tg}= 133 ns^{-1}.

In order to study the question of cooperativity between transitions of neighboring bonds we recorded the first passage time of the mth neighbor dihedral after the first transition of a central dihedral with m=1-4, instead of measuring the next transition time for the same dihedral. The central dihedrals are chosen as 5th to 10th of the n-heptadecane chain. In Figure 5 we show the hazard plots of these transition times at 296 K and characteristics of mth

Table 3. Characteristics of mth neighbor transitions

T(K)	c_1 (%)	c_2(%)	c_3 (%)	c_4 (%)	λ_1 (ns^{-1})	λ_2 (ns^{-1})	λ_3 (ns^{-1})	λ_4 (ns^{-1})
296	7.7	44.4	29.5	34.1	27.2	25.4	26.7	29.2
266	2.1	33.5	-	-	18.2	19.5	21.7	26.9
236	-	37.1	-	-	18.5	15.6	21.3	21.8
206	-	-	-	-	28.2	18.9	25.6	19.6

"-" represents negative values.

neighbor transitions at 296, 266, 236, and 206 K are listed in Table 3. This result is much similar to that of polymer conformation transition in the BD study.[3] The enhanced rate of transition of the second neighbors in a short time here is not so great as there, but it is greater than those of the other neighbors. It is also notable that the transition rate of the fourth neighbors is comparable with that of the second. The large value of c_2 implies that some 30% of the transitions of the second neighbors can be regarded as following transitions two bonds away in a correlated fashion. This correlation is related to the multiple transitions, discussed below.

The question of how often each type of several multiple transition such as crankshaft motion occur in the n-heptadecane molecular dynamics simulations at different temperatures is much interesting. For example, the stereoviews of "pair *gauche* production" of a n-heptadecane chain by ORTEP[19] is shown in Figure 6. Figure 6(a) shows the chain with a *gauche* state at the bond between sites 6 and 7, then after 41 time steps later the chain has one more *gauche* state at the bond between sites 8 and 9 (Figure 6(b)). Finally after 72 time steps there is another *gauche* state at the bond between sites 10 and 11 (Figure 6(c)). During these transitions, the ending sites, 1 and 17, hardly moved. To observe these multiple transitions, we looked at a short time period, τ (0.005 ns=10,000 time steps), in which the cooperative, second-neighbor pair transitions mostly occur. The central dihedrals for the multiple transitions are chosen for only 5th to 10th of the n-heptadecane chain.

In Table 4 are listed all such transitions and the number of times they occur in τ. Three-bond motions (*ttgtt* ⟷ *gtgtg*,

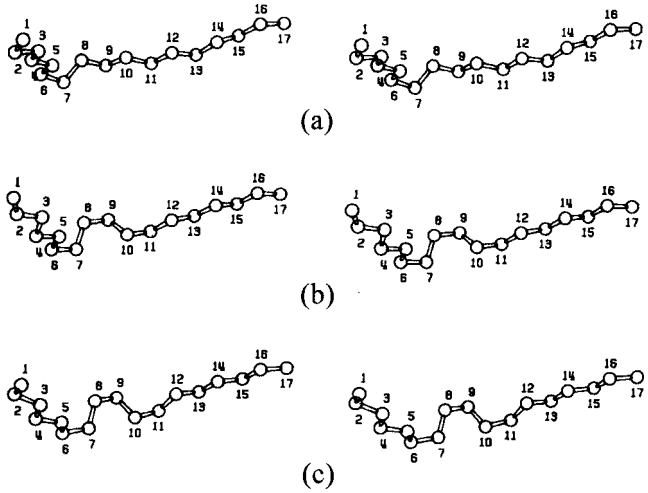

Figure 6. Stereoviews of "pair *gauche* production" as an example of multiple transitions.

Table 4. Numbers of each type of multiple transition in the initial 10,000 time steps

T(K)	total run	three-bond motion	*gauche* migration	pair *gauche* production
296	2,000 k	54	146	334
266	5,000 k	15	22	87
236	7,500 k	5	8	32
206	6,000 k	0	0	2

Figure 1(a)) are most rarely occurred since the transition *ttgtt* → *gtgtt* is easily occurred but the next transition *gtgtt* → *gtgtg* is less easier than the reversing transition *gtgtt* → *ttgtt*. *Gauche* migrations (*tgttt* ↔ *tttgt*, Figure 1(b)) are more frequently occurred than three-body motions. Here the transition *tgttt* → *tgtgt* is easily occurred but the next transition *tgtgt* → *tttgt* is less easier than the reversing transition *tgtgt* → *tgttt*. The activation of two barrier crossings in three-body motions is higher than that in *gauche* migration since the former is involved with three *gauche* production. Pair *gauche* productions (*ttttt* ↔ *tgtgt*, Figure 1(c)) are most frequently occurred in our MD study of *n*-heptadecane but in the BD study of polymer conformation transition[3] the two multiple transitions of type 2, *gauche* migration and pair *gauche* productions, are almost equally occurred. The reason for this difference remained unexplained except that it would probably come from the difference between the two methods, MD and BD.

Conclusion

We have carried out molecular dynamics (MD) simulations to investigate the conformational transition of liquid *n*-heptadecane at various temperatures. The behavior of the hazard plots for *n*-heptadecane obtained from our MD simulation is very similar to that of polymer conformation transition in a Brownian dynamics study[3] but the fractions of transition that immediately reverse are different. The transition rate at the ending dihedrals of the *n*-heptadecane chain is much higher than that at the central dihedrals. The enhanced rate of transition of the second neighbors in a short time is not so great as in the BD study,[3] but it is greater than those of the other neighbors. The large value of c_2 implies that some 30% of the transitions of the second neighbors can be regarded as following transitions two bonds away in a correlated fashion. In the analysis of multiple transitions, pair *gauche* production is most frequently occurred, and *gauche* migration and three-body motion are in order of the occurrence.

Acknowledgment. This research was supported by Basic Science Research Institute Program, Ministry of Education (BSRI-97-3414). SHL thanks the Korea Institute of Sciences and Technology for access to the Cray-C90 super computer and the Tongmyung University of Information Technology for access to its IBM SP/2 computers.

References

1. Skolnick, J.; Helfand, E. *J. Chem. Phys.* **1980**, *72*, 5489.
2. Helfand, E.; Skolnick, J. *J. Chem. Phys.* **1982**, *77*, 5714.
3. Helfand, E.; Wasserman, E. R.; Weber, T. A. *Macromolecules* **1980**, *13*, 526.
4. Helfand, E. *Science* **1984**, *226*, 647.
5. Pastor, R. W.; Venable, R. M.; Karplus, M. *J. Chem. Phys.* **1988**, *89*, 112.
6. Pastor, R. W.; Venable, R. M.; Karplus, M.; Szabo, A. *J. Chem. Phys.* **1988**, *89*, 1128.
7. Levy, R. M.; Karplus, M.; Wolynes, P. G. *J. Am. Chem. Soc.* **1981**, *103*, 5998.
8. Schatzki, T. F. *J. Polym. Sci.* **1962**, *57*, 496.
9. Monnerie, L.; Geny, F. *J. Chim. Phys.* **1969**, *66*, 1691.
10. Lee, S. H.; Kim, H. S. *Bull. Kor. Chem. Soc.* **1998**, *19*, 1068.
11. Chynoweth, S.; Klomp, U. C.; Scales, L. E. *Comput. Phys. Commun.* **199**, *62*, 297.
12. Chynoweth, S.; Klomp, U. C.; Michopoulos, Y. *J. Chem. Phys.* **1991**, *95*, 3024.
13. Berker, A.; Chynoweth, S.; Klomp, U. C.; Michopoulos, Y. *J. Chem. Soc., Faraday Trans.* **1992**, *88*, 1719.
14. Evans, D. J.; Hoover, W. G.; Failor, B. H.; Moran, B.; Ladd, A. J. C. *Phys. Rev.* **1983**, *A28*, 1016.
15. Simmons, A. D.; Cummings, P. T. *Chem. Phys. Lett.* **1986**, *129*, 92.
16. Ryckaert, J. P.; Bellemans, A. *Discuss. Faraday Soc.* **1978**, *66*, 95.
17. White, D. N. J.; Boville, M. J. *J. Chem. Soc., Perkin Trans.* **1977**, *2*, 1610,
18. Gear, C. W. *Numerical Initial Value Problems in Ordinary Differential Equation*; Englewood Cliffs NJ; Prentice-Hall, 1971.
19. Johnson, C. K. ORTEP. Report ORNL-3794; Oak Ridge National Laboratory: Oak Ridge, TN, 1972.